

## NEUROSCIENCE

# A cognitive process occurring during sleep is revealed by rapid eye movements

Yuta Senzai<sup>1,2\*</sup> and Massimo Scanziani<sup>1,2\*</sup>

Since the discovery of rapid eye movement (REM) sleep, the nature of the eye movements that characterize this sleep phase has remained elusive. Do they reveal gaze shifts in the virtual environment of dreams or simply reflect random brainstem activity? We harnessed the head direction (HD) system of the mouse thalamus, a neuronal population whose activity reports, in awake mice, their actual HD as they explore their environment and, in sleeping mice, their virtual HD. We discovered that the direction and amplitude of rapid eye movements during REM sleep reveal the direction and amplitude of the ongoing changes in virtual HD. Thus, rapid eye movements disclose gaze shifts in the virtual world of REM sleep, thereby providing a window into the cognitive processes of the sleeping brain.

**R**EM sleep is a phase of sleep characterized by rapid eye movements, from which it gets its acronym (1, 2). This phase of sleep is present across many vertebrates (3, 4) and has been associated with dreaming (5, 6). Indeed, when awakened during REM sleep, human subjects are more likely to report vivid dreams as compared to when they are awakened during other phases of sleep (7–10). This observation has led to the proposal that the nature of rapid eye movements during REM sleep may relate to the content of the ongoing dream (7–11). If so, rapid eye movements may represent a readout of some of the cognitive processes that occur in the sleeping brain. The verification of this hypothesis, however, has led to contradictory results. Some initial studies indicated a correlation between the content of dreams reported by the subject and the direction or frequency of rapid eye movements recorded immediately before awakening (7–10). However, other studies did not reproduce these results (12, 13). Furthermore, lifelong blind individuals who do not report visual experiences during dreams do have rapid eye movements during REM sleep (14). Thus, alternative hypotheses suggested that rapid eye movements may be unrelated to the mental processes that occur during REM sleep and simply reflect random brainstem activity (11, 15).

Most of these studies, however, were based on the potentially inaccurate reporting of dreams by human subjects rather than on an objective measure of the cognitive processes that occur in the brain during REM sleep. Thus, we reasoned that by directly monitoring some of the cognitive processes that occur in the brain during REM sleep, we could gain insight into whether rapid

eye movements actually occur in coordination with such processes.

We decided to use the head direction (HD) system of the mouse as the objective readout. HD cells are a population of neurons present, among other structures, in the anterodorsal nucleus of the thalamus (ADN). Their ensemble activity reports the direction of the head of the animal along the azimuth as it explores or navigates through its environment (16–18). During REM sleep, the population activity of HD cells is similar to that which occurs during actual navigation (19, 20), thus potentially representing an internal “virtual heading” of the sleeping animal.

In awake, behaving mice exploring their environment, changes in HD are accompanied by fast, saccade-like movements of the eyes in the same direction (21, 22). Does a similar coordination exist in the sleeping mouse? Clearly, a sleeping mouse maintains a fixed heading. However, putative changes in the internal representation of heading of the sleeping mouse may be coordinated with the rapid eye movements that occur during REM sleep. By monitoring rapid eye movements, we may be able to reveal changes in internal heading that are occurring in the virtual world of the sleeping brain.

We recorded from HD cells in the ADN of mice with extracellular linear probes while monitoring the movements of both eyes with head-mounted cameras (Fig. 1A and movies S1 and S2). Mice were free to explore an open-field arena, and their heading was monitored with a top-view camera (Fig. 1B). Mice were allowed to fall asleep, and their sleep phase was identified as REM or non-REM using standard electrophysiological parameters (animals spent 40 to 52% of the session asleep, and 10% of the sleeping period was identified as REM sleep; see table S1 and methods). To determine whether, during REM sleep, rapid eye movements are coordinated with the internal representation of heading, we proceeded through three steps: First, we established, in

awake mice, the relationship between saccade-like eye movements and the internal representation of the heading of the animal as decoded from the activity of HD cells (Fig. 1). Second, we determined the properties of rapid eye movements in mice during REM sleep (Fig. 2). Finally, we investigated the nature of the relationship between rapid eye movements in REM sleep and the internal representation of heading (Figs. 3 and 4).

We identified saccade-like eye movements in awake animals based on their fast dynamics ( $>400^\circ$  per second). During the exploration of the open-field arena, saccade-like eye movements occurred mainly along the nasotemporal axis (fig. S1, A and B), the vast majority (94.1%) of these eye movements were conjugated—that is, both eyes moved in the same direction, either clockwise (CW) or counterclockwise (CCW)—and the amplitude of these eye movements was correlated across eyes ( $R = 0.89$ ,  $P < 10^{-6}$ ; fig. S1C). Here, we focus on conjugated saccade-like eye movements of at least  $2^\circ$  in amplitude and refer to them simply as saccades. CW and CCW saccades were coupled to head turns in the same direction, that is, with CW and CCW head turns along the azimuth, respectively, consistent with previous reports (21, 22) (fig. S1, E and F). To determine the relationship between the direction of saccades and the internal representation of heading, we analyzed the population activity of HD cells recorded in the ADN while the animal explored the open-field arena (Fig. 1C and fig. S2, A and B). We recorded between 30 and 72 HD cells per animal ( $n = 6$  mice; table S1), which were defined as neurons whose activity was modulated by the heading of the animal along the azimuth (Fig. 1D and see methods). Using the heading of the animal and the simultaneously recorded HD cells, we trained an algorithm to report the heading solely based on the firing of HD cells (see methods). When tested on untrained periods of HD cell activity, the algorithm accurately decoded the heading of the mice as they explored their environment (Fig. 1E) with an error of only  $10.2^\circ \pm 3.5^\circ$  ( $n = 6$  mice; See fig. S2, C and D, and methods). How well does the direction of a saccade match the internal representation of a head turn? We quantified the internal representation of a head turn as the difference between the heading decoded 200 ms before and 200 ms after a saccade (Fig. 1F). The vast majority of saccades ( $95.2 \pm 1.3\%$ ,  $n = 6$  mice) occurred in the same direction (CW or CCW) as the ongoing head turns decoded from HD cell activity (Fig. 1, G and H). In awake animals, saccade direction and the internal representation of head turns are thus tightly coupled.

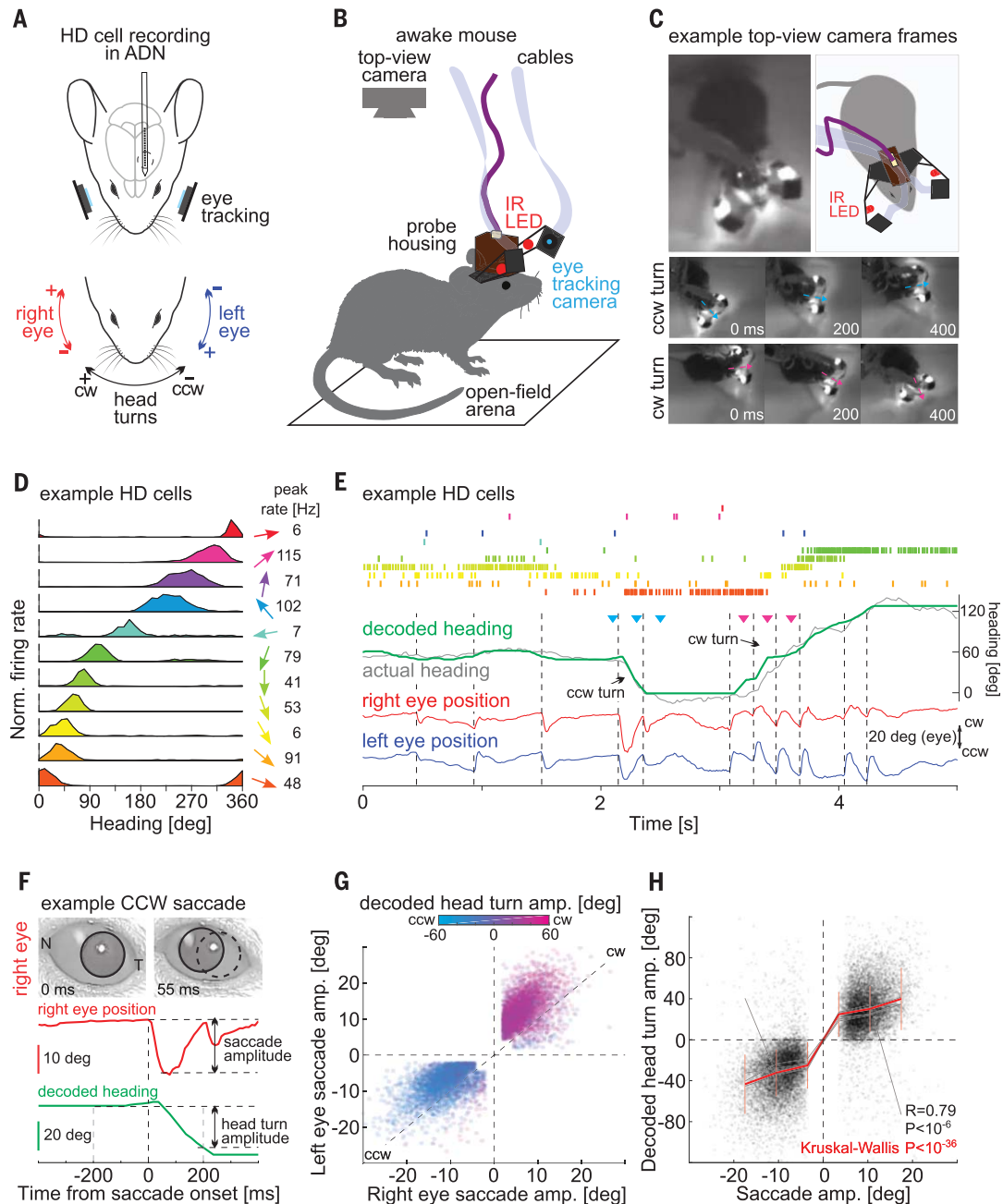
Is this relationship maintained during REM sleep? To monitor rapid eye movements during REM sleep, we took advantage of the fact that

<sup>1</sup>Department of Physiology, University of California, San Francisco, San Francisco, CA, USA. <sup>2</sup>Howard Hughes Medical Institute, University of California, San Francisco, San Francisco, CA, USA.

\*Corresponding author. Email: yuta.senzai@gmail.com (Y.S.); massimo@ucsf.edu (M.S.)

**Fig. 1. Saccade direction predicts internal representation of head turns.**

**(A)** Schematic of the experimental configuration illustrating a chronic electrophysiological recording from the ADN while eye and head movements are monitored with cameras. **(B)** Schematic illustration of the open-field arena with a mouse carrying head-mounted eye cameras and silicon probes. The heading of the animal is monitored with a top-view camera. IR LED, infrared light-emitting diode. **(C)** An example frame from the top-view camera is shown at the top left, and a schematic illustration of the frame is shown at the top right. The top and bottom middle panels present example frames showing a CCW turn and a CW turn, respectively. Arrows indicate the heading of the animal in each frame. **(D)** The tuning curves of 11 example HD cells recorded from the ADN of an awake mouse. The arrows on the right indicate the preferred HD of each HD cell. Peak firing rates for HD cells are shown on the right. **(E)** Shown at the top is a raster plot of the firing of the 11 example HD cells shown in (D). Middle traces illustrate the actual heading of the animal (gray) and heading decoded from the population activity of HD cells (green). Triangles mark the timing of example frames for the CCW turn (cyan) and CW turn (magenta) shown in (C). Bottom traces illustrate the horizontal position of the two eyes (red and blue). The vertical dashed lines indicate the onset of saccades. **(F)** Two snapshots of the right eye taken before and after a CCW saccade are shown at the top. The pupil is delineated with a black circle. A dashed circle in the right image labels the pupil's original position (N, nasal commissure; T, temporal commissure). The red trace illustrates the right eye's horizontal position in time. Saccade amplitude was defined as the change in the horizontal eye position upon a saccade. The green trace illustrates the decoded heading. The head-turn amplitude is the change in the decoded heading between 200 ms before and 200 ms after saccade onset. Note the CCW shift in decoded heading concomitant with the CCW saccade. **(G)** Summary scatter plot of the amplitude of conjugated saccades during the



mice do not always close their eyes while asleep (Fig. 2, A and B, and movie S2). We quantified the direction and amplitude of rapid eye movements in the sleeping animal using the head-mounted cameras (23, 24). During REM sleep

(Fig. 2C and see methods), rapid eye movement occurred along the nasotemporal axis (monitored over a total of 68 min of REM sleep in six mice; fig. S3, A and B), and the direction of these movements, CW or CCW, was well correlated

exploration in the open field arena ( $n = 13,778$  from six mice). The amplitude and sign of the decoded head turn during the saccade are color coded. Note that the direction of the saccades matches the direction of the decoded head turn. In this and the rest of the figures, the upper-right and lower-left quadrants of the scatter plots represent CW and CCW movements, respectively. **(H)** Correlation between the amplitude of conjugated saccades (averaged over both eyes) and the decoded head-turn amplitude. Saccade amplitude predicted the amplitude of decoded head turns for each individual mouse (gray lines) as well as for all mice (red line; vertical lines represent standard deviation).

across both eyes ( $R = 0.58$ ,  $P < 10^{-6}$ ; Fig. 2, C to E), thus similar to saccades observed in awake animals (fig. S3C), albeit with smaller amplitudes (average amplitude:  $5.1^\circ \pm 2.5^\circ$  for rapid eye movements and  $9.7^\circ \pm 3.5^\circ$  for saccades) and

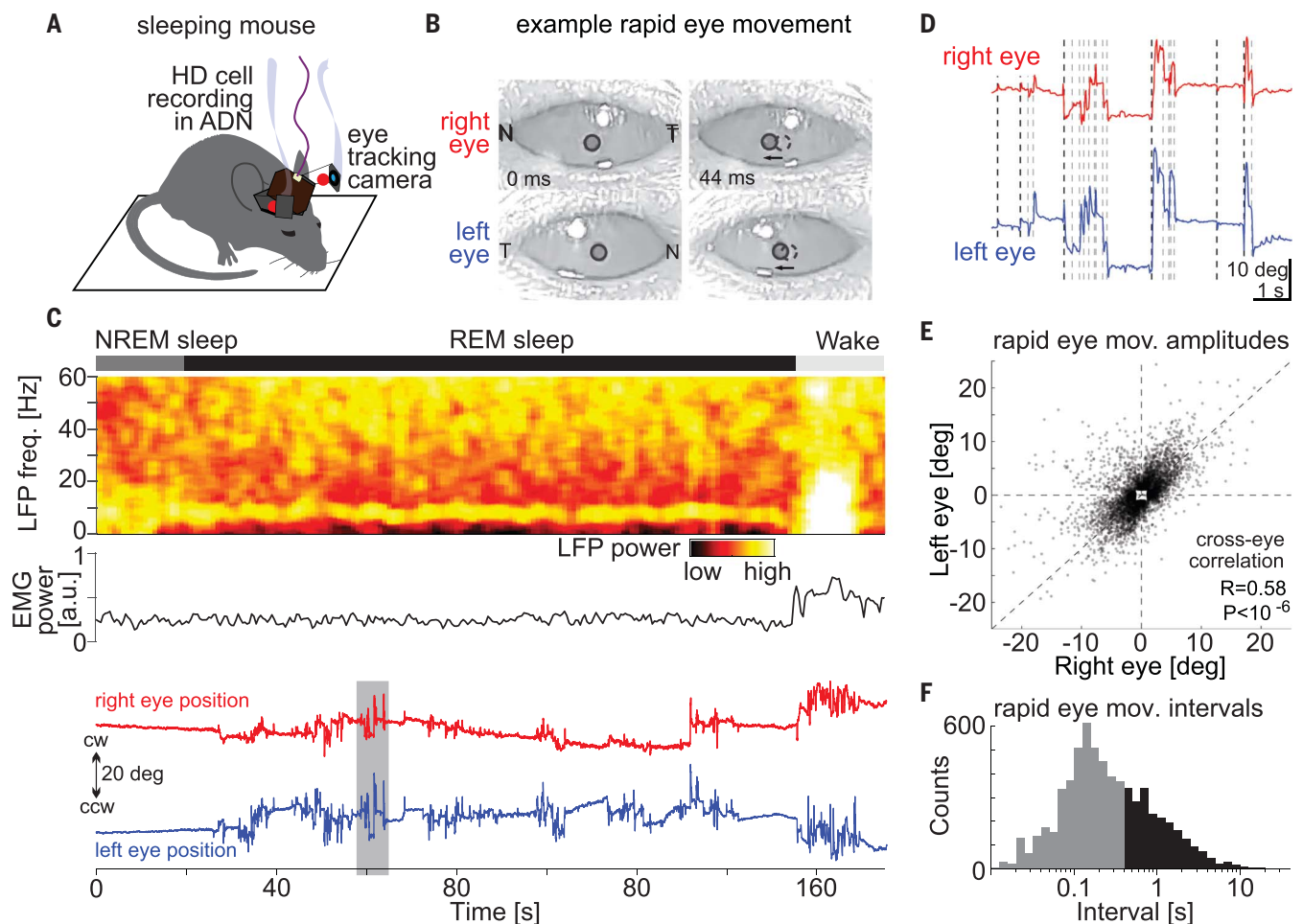


**Fig. 2. Rapid eye movements during REM sleep.** (A) Schematic of the experimental configuration illustrating a chronic electrophysiological recording from the ADN while rapid eye movements are monitored with cameras in a sleeping mouse. (B) Snapshots of the right (top) and left (bottom) eye before (left) and after (right) a CCW rapid eye movement. The pupil is delineated with a black circle. A dashed circle in the right image labels the pupil's original position. Note that both eyes move CCW. (C) An example spectrogram of the local field potential (LFP) recorded in the ADN during non-REM sleep (NREM), REM sleep, and wakefulness (Wake) is shown at the top. Electromyography (EMG) power is shown in the middle. The horizontal position of the two eyes (red and blue) is shown at the bottom. Note the increase in eye movements at the

onset of REM sleep. a.u., arbitrary units. (D) The shaded time interval in (C) shown on an expanded time scale. Note that for most rapid eye movements, both eyes moved to the same direction. Dashed black and gray vertical lines indicate the onset of leading (not preceded by a rapid eye movement for at least 400 ms) and follower rapid eye movements. (E) Scatter plots of the amplitude of right versus left rapid eye movements during REM sleep for all mice ( $n = 6689$  from six mice). Note that most data points are in the lower-left or upper-right quadrants, indicating CCW and CW movements of both eyes. (F) Distribution of intervals between rapid eye movements during REM sleep for all mice ( $n = 6689$  from six mice). Leading eye movements are in black, and followers are in gray.

at higher frequency (median interval: 267 ms for rapid eye movements and 521 ms for saccades; Fig. 2F and fig. S1D).

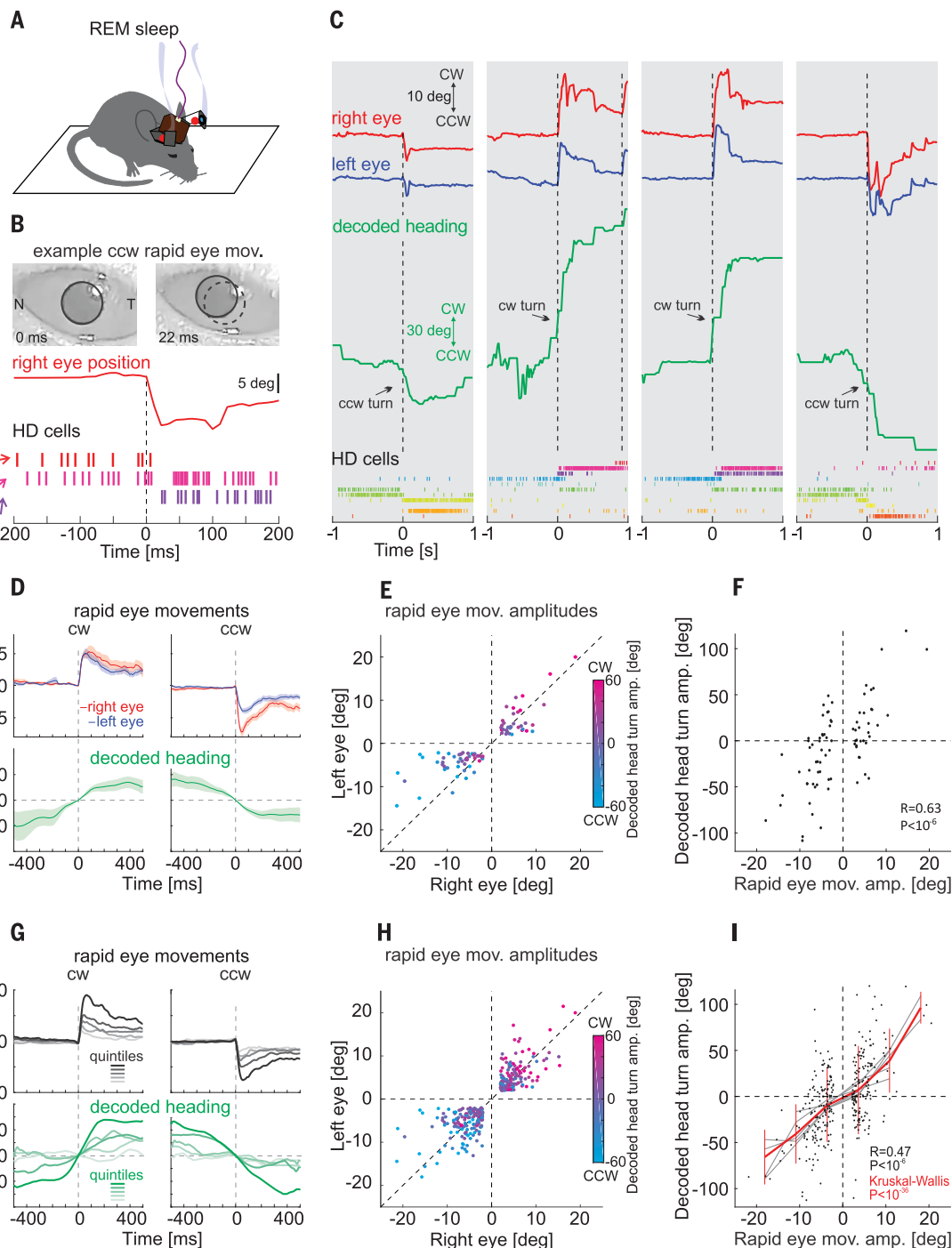
We decoded the internal representation of heading during REM sleep, that is, the virtual heading, by applying the algorithm described above. Virtual heading was decoded from the activity of the same set of HD cells that was used to train the algorithm, this time, however, recorded during REM sleep. Changes in virtual heading, that is, virtual turns, occurred with an angular velocity that was similar to that decoded during actual turns in awake mice exploring the arena (fig. S4, A and B), consistent with previous results (19). Further-

more, during REM sleep, HD cells maintained a similar correlational structure as that observed during wakefulness: HD cells that either fired or did not fire together in wakefulness exhibited the same pattern during REM sleep (fig. S4, C and D). To test the relationship between rapid eye movements and virtual heading, we first focused our analysis on rapid eye movements that were not preceded by any eye movement for at least 400 ms (Fig. 2F) and in which both eyes moved by at least  $2^\circ$  in the same direction (i.e., conjugated rapid eye movements; see methods). This allowed us to have a sufficiently long baseline to detect potential changes in virtual heading that were specif-

ically associated with the selected conjugated rapid eye movements. We refer to these rapid eye movements as “leading” eye movements. The direction of leading rapid eye movements matched the direction of simultaneously recorded virtual turns (Fig. 3, A to C). A CCW leading rapid eye movement, for example, occurred as the ensemble activity of HD cells shifted CCW (Fig. 3B), and vice versa (Fig. 3C). Overall, during REM sleep, the direction of leading rapid eye movements predicted the direction of the changes in virtual heading, both in each individual mouse (Fig. 3, D to F, and fig. S5) as well as in the population (Fig. 3, G and H). Furthermore, not only the direction

### Fig. 3. Leading rapid eye movements predict decoded head turns during REM sleep.

**(A)** Schematic of the experimental configuration (same as Fig. 2A). **(B)** Two snapshots of the right eye during REM sleep taken before and after a CCW rapid eye movement are shown at the top. The red trace illustrates the right eye's horizontal position in time. A raster plot of the firing of three example HD cells (out of the 11 HD cells illustrated in Fig. 1D, with the same color coding) is shown at the bottom. Note the CCW shift in heading representation concomitant with the CCW rapid eye movement. **(C)** Four example episodes illustrating a concomitant shift in decoded heading and eye position during REM sleep. The top traces illustrate the horizontal position of the two eyes (red and blue) and decoded heading (green). The vertical dashed lines indicate the onset of leading rapid eye movements. Shown at the bottom is a raster plot of the firing of the 11 example HD cells (same as in Fig. 1D). **(D)** The average relative position of the right (red) and left (blue) eyes for CW (left) and CCW (right) leading eye movements is shown at the top. The average decoded heading (green) is shown at the bottom. Shaded areas are standard error of the mean [average of 34 traces for CW and 47 traces for CCW leading eye movements]. **(E)** Scatter plot of the amplitude of leading right versus left eye movements during REM sleep. The amplitude and sign of the decoded head turns during the eye movements are color coded. Note the good match between the direction of the rapid eye movements and the direction of the decoded head turn. **(F)** Correlation between the amplitude of leading eye movements during REM sleep (averaged over both eyes) and the decoded head-turn amplitude. For (B) to (F), the representative mouse is the same as that in Fig. 1, C to E. **(G)** Mean traces of horizontal eye position averaged across both eyes for CW (left) and CCW (right) leading eye movements ( $n = 6$  mice) are shown at the top. The dataset was separated into quintiles based on the amplitude. Mean traces of the decoded heading in each quintile based on the



amplitude of leading rapid eye movements are shown at the bottom. Note that leading rapid eye movements with larger amplitude coincide with larger decoded head turns. **(H)** Summary scatter plot of the amplitude of leading right versus left eye movements during REM sleep ( $n = 330$  from six mice). The amplitude and sign of the decoded head turns during the eye movements are color coded. **(I)** Correlation between the amplitude of leading eye movements during REM sleep and the decoded head-turn amplitude ( $n = 330$  from six mice). Leading rapid eye movements predicted the direction and amplitude of decoded head turns in each individual mouse (gray lines) as well as for all mice (red line; vertical lines indicate standard deviation).

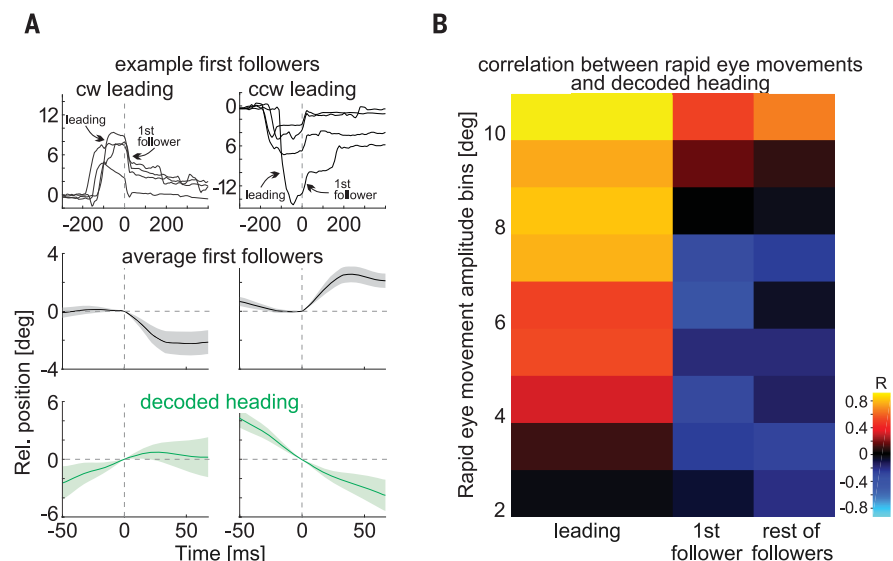


**Fig. 4. Small-amplitude follower eye movements represent recentering eye movements.** (A) Example traces of horizontal eye position (averaged across both eyes) aligned to the onset of first follower rapid eye movement after a CW (left) and CCW (right) leading eye movement are shown at the top. Average relative positions (mean of both eyes) for first follower eye movements after CW (left) and CCW (right) relative movement (average over 132 traces for CW and 107 traces for CCW from six mice) are shown in the middle. Average traces of concomitantly decoded heading are shown at the bottom. Note that, on average, first followers occur in the opposite direction as compared to the preceding leading eye movement and to the decoded head turn. Shaded areas represent standard error of the mean. The time scale of the top panels covers a larger interval to include the preceding leading eye movement. (B) Correlation (heatmap) between the decoded head-turn amplitude and amplitude of rapid eye movement (in bins; averaged for both eyes; y axis). The first column from the left shows leading eye movements ( $n = 330$  from six mice), the second column shows first followers ( $n = 239$  from six mice), and the third column shows the rest of the followers ( $n = 970$  from six mice). Note the increased positive correlation with increasing eye movement amplitude.

of the leading eye movements but also their amplitude provided information about the ongoing internal representation of heading: the larger the amplitude of the leading rapid eye movement, the larger the angle of the simultaneously recorded virtual turn (Fig. 3, G to I).

What is the relationship between rapid eye movements that follow leading eye movements and the virtual heading of the animal? We refer to these eye movements as “followers,” that is, those that occur less than 400 ms after another rapid eye movement. The above results (top panels of Fig. 3, D and G) show that the average position of the eye following a leading eye movement progressively returns to the original position occupied before the leading movement, as if recentering the eye [400 ms after a leading eye movement, the eye returned to  $34.1 \pm 3.3\%$  (mean  $\pm$  SEM) relative to its peak position after the leading eye movement]. By contrast, the simultaneously decoded virtual heading did not (bottom panels of Fig. 3, D and G). If the recentering of the eye is mediated by followers, the direction of these rapid eye movements should be opposite relative to that of leading eye movements and to the ongoing changes in virtual heading. Indeed,

the direction of followers that occur immediately after a leading eye movement (first followers) were, on average, opposite to the direction of the preceding leading eye movement (Fig. 4A and fig. S6A) and thus opposite to the direction of the ongoing head turns (Fig. 4, A and B, and fig. S6, B and C). Overall, the direction of followers was opposite to the direction of changes in virtual heading, but for the small fraction of followers (4.3%) with the largest amplitudes ( $>10^\circ$ ; Fig. 4B and fig. S6, D and E) that, like leading eye movement, matched the directions of virtual head turns.

Taken together, these data demonstrate a tight relationship between rapid eye movements and the internal representation of the heading of the animal during REM sleep (Fig. 4B). Not only does the direction of leading rapid eye movements predict the direction of change in virtual heading, but their amplitude predicts the magnitude of the change. Conversely, follower eye movements recenter the eye. Thus, our results demonstrate that rapid eye movements provide a readout of the internal representation of heading in the sleeping brain. The coordination between rapid eye movements during REM sleep and the HD system

suggests that shifts in virtual heading are part of a globally orchestrated representation of “virtual navigation” by the sleeping brains rather than the result of some uncorrelated random walk of the HD system (20).

How do eye movements that occur during REM sleep map onto eye movements observed during wakefulness? Leading rapid eye movements may correspond to saccades because both match the direction of the ongoing head turn, virtual or real (21, 22, 25). Follower eye movements, however, appear unlike any eye movement in the awake animal. In the awake mouse, the recentering of the eye after a saccade is mediated by image stabilizing reflexes—the vestibular and optokinetic reflexes—that are engaged by the ongoing head turn (21, 22, 25). In the sleeping, motionless animal, however, the sensory periphery that triggers these reflexes is not engaged. It is conceivable that recentering eye movements during REM sleep may still be triggered by activity in the vestibular nuclei. Such activity, although independent of the sensory periphery, could be part of the globally orchestrated virtual navigation mentioned above.

Whether rapid eye movements in REM sleep reveal the subjects’ direction of gaze in the imagery of dreams has been debated since the discovery of this sleep phase and its association with vivid dreams (7–13). Because of the lack of objective measures that assess the content of dreams, initial studies have led to conflicting results, leading to the conclusion that rapid eye movements are likely uncorrelated with the cognitive activity of the sleeping brain (12, 13). More recently, studies performed on human patients or animal models that partially enact their dreams because of reduced muscle atonia during REM sleep have led to a reevaluation of the original hypothesis (26, 27). In these studies, at least some rapid eye movements appeared to be coordinated with the direction of the behavior enacted during REM sleep. However, the extent to which the coordination between eye and body movement is a result of the pathological or experimentally reduced atonia still remains unclear.

By harnessing the HD system of the rodent and the correlation between orienting head and eye movements in awake animals, we have established a clear relationship between changes in virtual heading and rapid eye movements during REM sleep. Thus, our results indicate that rapid eye movements provide an external readout of an internal cognitive process that is occurring during REM sleep, namely the change in virtual heading. Our results further suggest the existence of a globally coordinated activity among distinct systems in the sleeping brain during REM sleep, a coordination that may underlie the realistic and vivid experience of dreams. Understanding the neurophysiological mechanisms of this coordination will give us

# insight into the organization of the brain's generative model of the world (28, 29).

## REFERENCES AND NOTES

1. E. Aserinsky, N. Kleitman, *Science* **118**, 273–274 (1953).
2. M. Jouvet, *Prog. Brain Res.* **18**, 20–62 (1965).
3. M. S. Blumberg, J. A. Lesku, P.-A. Libourel, M. H. Schmidt, N. C. Rattenborg, *Curr. Biol.* **30**, R38–R49 (2020).
4. J. B. Jaggard, G. X. Wang, P. Mourrain, *Curr. Opin. Neurobiol.* **71**, 44–51 (2021).
5. J. A. Hobson, *Nat. Rev. Neurosci.* **10**, 803–813 (2009).
6. Y. Nir, G. Tononi, *Trends Cogn. Sci.* **14**, 88–100 (2010).
7. W. Dement, N. Kleitman, *J. Exp. Psychol.* **53**, 339–346 (1957).
8. H. P. Roffwarg, W. C. Dement, J. N. Muzio, C. Fisher, *Arch. Gen. Psychiatry* **7**, 235–258 (1962).
9. R. J. Berger, I. Oswald, *Science* **137**, 601 (1962).
10. J. H. Herman *et al.*, *Sleep* **7**, 52–63 (1984).
11. I. Arnulf, *Arch. Ital. Biol.* **149**, 367–382 (2011).
12. E. Moskowitz, R. J. Berger, *Nature* **224**, 613–614 (1969).
13. L. Jacobs, M. Feldman, M. B. Bender, *Psychophysiology* **9**, 393–401 (1972).
14. N. H. Kerr, D. Foulkes, M. Schmidt, *J. Nerv. Ment. Dis.* **170**, 286–294 (1982).
15. G. Vanni-Mercier, G. Debilly, *Neuroscience* **86**, 571–585 (1998).
16. J. B. Ranck, *Soc. Neurosci. Abstr.* **10**, 599 (1984).
17. J. S. Taube, R. U. Muller, J. B. Ranck Jr., *J. Neurosci.* **10**, 436–447 (1990).
18. J. S. Taube, *J. Neurosci.* **15**, 70–86 (1995).
19. A. Peyrache, M. M. Lacroix, P. C. Petersen, G. Buzsáki, *Nat. Neurosci.* **18**, 569–575 (2015).
20. R. Chaudhuri, B. Gerçek, B. Pandey, A. Peyrache, I. Fiete, *Nat. Neurosci.* **22**, 1512–1520 (2019).
21. A. F. Meyer, J. O'Keefe, J. Poort, *Curr. Biol.* **30**, 2116–2130.e6 (2020).
22. A. M. Michaiel, E. T. Abe, C. M. Niell, *eLife* **9**, e57458 (2020).
23. Ö. Yüzgeç, M. Prsa, R. Zimmermann, D. Huber, *Curr. Biol.* **28**, 392–400.e3 (2018).
24. G. Ungurean, D. Martinez-Gonzalez, B. Massot, P. A. Libourel, N. C. Rattenborg, *Curr. Biol.* **31**, 5370–5376.e4 (2021).
25. J. H. Fuller, *Vision Res.* **25**, 1121–1128 (1985).
26. L. Leclair-Visonneau, D. Oudiette, B. Gaymard, S. Leu-Semenescu, I. Arnulf, *Brain* **133**, 1737–1746 (2010).
27. K. Soh, Y. Morita, H. Sei, *Physiol. Behav.* **52**, 553–558 (1992).
28. G. E. Hinton, P. Dayan, B. J. Frey, R. M. Neal, *Science* **268**, 1158–1161 (1995).
29. J. A. Hobson, C. C.-H. Hong, K. J. Friston, *Front. Psychol.* **5**, 1133 (2014).
30. Y. Senzai, M. Scanziani, A cognitive process occurring during sleep is revealed by rapid eye movements. Dryad (2022); <https://doi.org/10.7727/Q6P26WDC>.

## ACKNOWLEDGMENTS

We thank M. Mukundan, P. Saraf, B. Wong, and L. Bao for technical assistance; the former and current members of the Scanziani labs for discussions and comments; and R. A. Nicoll for comments on the manuscript. We thank J. Schor for help with the head-mounted camera system. M.S. was previously granted a CC BY 4.0 license to the public and a sublicensable license to Howard Hughes Medical Institute (HHMI) in his research articles pursuant to which M.S. has the right to make the author-accepted manuscript of his articles immediately available upon publication, and any rights M.S. grants in his research articles are subject to

the public and HHMI licenses. **Funding:** This work was funded by National Institutes of Health grants U19NS107613 (M.S.) and R01EY025668 (M.S.), the Howard Hughes Medical Institute (M.S.), and the Japan Society for the Promotion of Science (Y.S.).

**Author contributions:** Y.S. and M.S. designed the study. Y.S. conducted all experiments and analyses. Y.S. and M.S. wrote the paper. **Competing interests:** The authors declare that they have no competing interests. **Data and materials availability:** All data and analyses necessary to understand and assess the conclusions of the manuscript are presented in the main text and in the supplementary materials. Data and codes will be publicly available at Dryad (30). **License information:** Copyright © 2022 the authors, some rights reserved; exclusive licensee American Association for the Advancement of Science. No claim to original US government works. <https://www.science.org/about/science-licenses-journal-article-reuse>. This research was funded in whole or in part by HHMI, a cOAlition S organization. The author will make the Author Accepted Manuscript (AAM) version available under a CC BY public copyright license.

## SUPPLEMENTARY MATERIALS

[science.org/doi/10.1126/science.abp8852](https://science.org/doi/10.1126/science.abp8852)

Materials and Methods

Figs. S1 to S6

Table S1

References (31–38)

MDAR Reproducibility Checklist

Movies S1 and S2

[View/request a protocol for this paper from Bio-protocol.](#)

Submitted 3 March 2022; accepted 7 July 2022

10.1126/science.abp8852

## A cognitive process occurring during sleep is revealed by rapid eye movements

Yuta SenzaiMassimo Scanziani

*Science*, 377 (6609), • DOI: 10.1126/science.abp8852

### The meaning of rapid eye movement

Sleep includes phases characterized by rapid eye movement (REM) that were known to be associated with dreaming. But are these eye movements related to the contents of consciousness in that sleep state? Senzai and Scanziani recorded head direction cells in the anterior dorsal nucleus of the thalamus in mice during wake and sleep (see the Perspective by De Zeeuw and Canto). The direction and amplitude of rapid eye movements encoded the direction and amplitude of the heading of mice in their virtual environment during REM sleep. It was possible to predict the actual heading in the real and virtual world of the mice during wake and REM sleep, respectively, using saccadic eye movements. —PRS

### View the article online

<https://www.science.org/doi/10.1126/science.abp8852>

### Permissions

<https://www.science.org/help/reprints-and-permissions>

Use of this article is subject to the [Terms of service](#)